

THERMAL EFFECTS IN HYDRODYNAMIC JOURNAL BEARINGS OF SPEED INCREASING AND REDUCTION GEARBOXES

by

Christophe Bouchoule

Postdoctoral Researcher

Michel Fillon

CNRS Researcher

Daniel Nicolas

Professor of Mechanics

Université de Poitiers

Laboratoire de Mécanique des Solides

Poitiers Cedex, France

and

Franck Barresi

Flender Graffenstaden

Illkirch Cedex, France

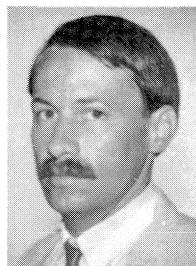


Christophe Bouchoule is a Postdoctoral Researcher at the Laboratory of Solid Mechanics of the University of Poitiers in France, where he obtained his Doctorate in the field of Mechanics (1994). For three years, he has worked in the field of Tribology, with the contact mechanics team directed by Professor J. Frêne and in the framework of a contract with an industrial partner. His major research interests are thermal effects in high speed plain and tilting-pad journal

bearings. These bearings are used in speed increasing and reduction gearboxes for power applications with regard to experiments.



Daniel Nicolas has been Professor of Mechanics at the University of Poitiers since 1985. From 1975 to 1985, he was researcher and teacher at Insa of Lyon (Laboratory of Contact Mechanics) where he obtained his Doctorate. Dr. Nicolas has worked in the fields of both hydrodynamic and hydrostatic lubrication for 25 years.



Michel Fillon studied in the field of Mechanics at the University of Poitiers in France where he obtained his Doctorate studying thermal effects in hydrodynamic bearings. After two years working as engineer in the field of Lumbering Mechanization Research, he rejoined the Laboratory of Solid Mechanics at the University of Poitiers. In this Laboratory, he has been a CNRS Researcher since 1988. He has worked in the field of Tribology in the contact mechanics team

directed by Pr. J. Frêne. Current research interests are both experimental and theoretical investigations of hydrodynamic bearings. Dr. Fillon has been principal author or co-author of about 15 international papers in this field, principally on thermal effects in plain and tilting-pad journal bearings. He is responsible with Pr. J. Frêne and Pr. D. Nicolas, for the direction of the research works Doctoral students at the University of Poitiers. He works frequently with industrial partners to solve concrete problems on journal and thrust bearings for turbomachinery. He is also a member of STLE.

ABSTRACT

The objective of this work is to minimize the maximum bearing temperatures under severe operating conditions in speed increasing and reduction gearboxes, and to present experimental data to validate the theoretical assumptions. The test machine, the experimental results, and the comparison between theoretical thermoelastohydrodynamic results and experimental data are presented. The test bearings are located in two speed increasing and reduction gearboxes (back-to-back test bed). The high speed shaft bearings are five shoe tilting-pad journal bearings. They are 160 mm in diameter and the bearing ratio (L/D) is equal to 1.0. The rotational speed varies from 2700 rpm (22 m/s) to 11,880 rpm (100 m/s). The applied load is up to 88 kN. Three types of bearings permit analyzing the influence of the bearing design and the pivot position on the pad. The low speed rotor bearings are offset-halves journal bearings. They are 230 mm in diameter and the bearing ratio is equal to 0.75. The rotational speed varies from 765 rpm (9.0 m/s) to 3366 rpm (40 m/s). The applied load is up to 100 kN. The influence of the load direction and of the oil feeding temperature is studied. For each test, bearings, temperatures (film/pad interface, oil, pad and housing), power losses and oil flow are measured. Shifting the pivot from the central position to at least the 55 percent position leads to a decrease of the maximum temperature. The bearing design

and materials contribute to improve its performance, especially a decrease of maximum temperature and power loss.

INTRODUCTION

This research is carried out in the framework of a contract between the Laboratory of Solids Mechanics of Poitiers and the Flender-Graffenstaden company. This society is designing and manufacturing increasing and reduction gearboxes for high-speed applications such as turbine/generator or motor/compressor/pump.

The bearings of these mechanisms are essential parts and are usually used. They have very high operating speeds ($V > 90$ m/s) and large loads. Because the machines run with low viscosity mineral oil, the severe conditions in the high-speed drive trains of these machines induce babbitt temperatures close to 130°C .

The most common problem with bearings in industrial gearboxes is excessive operating temperature. Thus, it is of interest to determine under which conditions the bearing temperature can be minimized. The apparatus used permits operation under conditions close to those usually applied in practice. The apparatus permits measurements of bearings element temperatures (babbitt, pads, housing, and oil baths) along with other parameters such as oil flowrate and shaft vibrations. Five-shoe tilting-pad journal bearings are used in the high speed shaft (HSS), because they are particularly appropriate for high-speed applications and have excellent dynamic characteristics. For the low speed shaft (LSS), offset-halves bearings are used.

Because of increasing severe operating conditions in tilting-pad journal bearings, thermal effects, and thermoelastic deformation of bearing elements have been taken into account in recent theoretical models [1, 2]. Most authors have compared their theoretical results only with steady-state operating characteristics and usually for only one tilting-pad journal bearing. Most of experimental data [3, 4, 5, 6, 7, 8, 9, 10] have been realized with laboratory apparatus. To validate the models, however, it is necessary to have more exhaustive experimental data obtained on industrial apparatus.

For very high speeds, the thermal effects are important but, alone, they cannot accurately predict the bearing performance. For high operating speeds, for example, the effects of the nonlaminar flow regime effects must be taken into account. Gardner and Ulschmid [11] experimentally studied both a tilting-pad and a sleeve journal bearing. They showed that the change in flow regime from laminar to turbulent leads to the reduction of the maximum temperature and to a drastic increase of the power losses. More recently, Hopf and Schuler [5] presented experimental results obtained for journal bearings that operate in transition between laminar and turbulent flow regime. They demonstrated that the change in flow regime leads to a local diminution of the babbitt temperature only near the minimum film thickness, but the temperature in the other zones increased with the rotational speed. They also noted a change in the bearing behavior at a constant speed: when the load increased, above a certain limit, the surface temperatures jumped upwards. Taniguchi, et al. [6], observed a large tilting-pad journal bearing for a very good agreement between theoretical and experimental results. Recently, Bouard, et al. [12], studied three thermohydrodynamic turbulent models applied to tilting-pad journal bearings. A local analysis of thermal turbulent phenomena was shown. During the change in flow regime, the inconsistency between the increase of power losses and the decrease of maximum temperature when the rotational speed increases is explained using the velocity profile. In fact, the theoretical analysis shows that the average temperature in the film always increases with the rotational speed. Finally, Simmons and Dixon [10] presented the results of a wide ranging program of experi-

mental work with a 200 mm diameter, five-shoe tilting-pad journal bearing. One of the most interesting features of their results is the significant effect on pad temperature of an apparent laminar to turbulent transition regime in the film that occurs at high operating speeds. Their experimental results suggested that a transition from laminar to turbulent cooling may occur in the surrounding oil flow rather than in the hydrodynamic film.

TEST APPARATUS

The test rig used for the experimental work is shown in Figure 1 to illustrate the principle of a back-to-back test bed. It consists of two identical gearboxes (machine A and machine B), which are mechanically coupled one to the other, pinion to pinion and gear to gear which form a kinematic chain. With the single helical teeth, the gears can be loaded up to the full load just by applying an axial force on the high speed shaft. The axial shifting causes a rotary movement and the required closed torque circuit between the two gears is established.

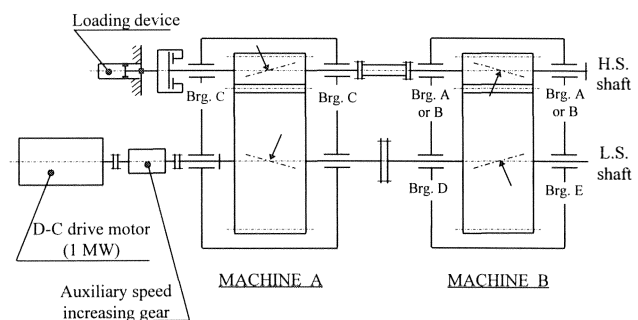


Figure 1. Back-to-Back Test Bed.

The axial force is produced by means of a hydraulic piston. The apparatus is driven by a 1.0 MW dc motor capable of providing rotational speeds up to 1800 rpm, coupled at the extremity of the low speed shaft. By this arrangement and at nominal running conditions ($P = 3.5$ MPa; $N = 10800$ rpm), the transmitted power from one machine to the other is 21 MW. A comprehensive view of the back-to-back test bed is given on the photograph in Figure 2.

EXPERIMENTAL BEARING

The characteristics at 20°C of the HSS bearings used in this experimental work are given in Table 1 for the three bearings

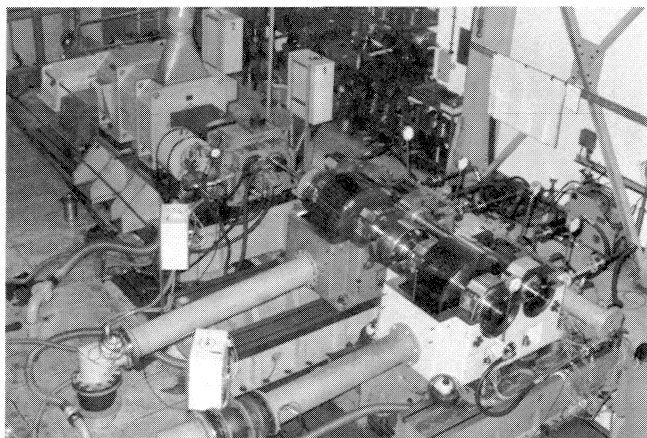


Figure 2. General View of the Experimental Device.

Table 1. HSS Bearing Geometry and Operating Conditions.

		Bearing A	Bearing B	Bearing C
Number of pads		5	5	5
Journal diameter	(m)	0.16	0.16	0.16
	in	6.299	6.299	6.299
Bearing length	(m)	0.16	0.16	0.16
	in	6.299	6.299	6.299
Radial bearing clearance	(m)	$0.145 \cdot 10^{-3}$	$0.145 \cdot 10^{-3}$	$0.145 \cdot 10^{-3}$
	in	0.0057	0.0057	0.0057
Pad thickness	(m)	$22 \cdot 10^{-3}$	$22 \cdot 10^{-3}$	$22 \cdot 10^{-3}$
	in	0.886	0.886	1.063
Load direction		Between pads	Between pads	Between pads
Pad arc angle	(°)	60	60	60
Pivot position on pad		0.5	0.55	0.6
Applied load	(kN)	0 to 88	0 to 88	0 to 88
	lb	zero to 19,500	zero to 19,500	zero to 19,500
Range of speed	(rpm)	0 to 12,400	0 to 12,400	0 to 12,400
Oil inlet temperature	(°C)	50 and 72	50 and 72	50 and 72
	°F	122 and 161.6	122 and 161.6	122 and 161.6

tested. The journal diameter is 160 mm and aspect ratio L/D is equal to 1.0. The pads of the bearings A and B are steel backed, lined with tin base whitemetal; they have respectively a center ($\alpha/\beta = 0.5$) and offset pivots ($\alpha/\beta = 0.55$) on their reverse sides (typical "rocker back" pivot). For bearing C, the material of the housing pads is a copper-bronze alloy, lined with the same base whitemetal as the two other bearings. Each pivot consists of a spherical "mushroom" with a hardened head held rigidly to the casing of the bearing. The pivot works in conjunction with a spherical seat, machined in the back of the pad. The shaft and housing are case-hardening steel and mild steel, respectively. The oil was supplied to the bearings using directed lubrication by means of gauged nozzles located between pads, with a supply pressure of 0.15 MPa. The oil inlet temperature and lubricant pressure of each bearing were individually measured. In addition, the oil drain temperature of each bearing was also measured.

The offset-halves bearing geometry and operating conditions are given in Table 2 for two of the bearings tested. The journal diameters of bearing D and bearing E are 230 mm, and the bearing ratio is equal to 0.75. They are steel backed, lined with tin base whitemetal. Oil feed is realized by twin axial grooves located at 90 degrees to the load line, under a supply pressure of 0.1 MPa.

The flowrate of all the bearings was also measured to within 1.0 percent using flowmeters. The rotational speed was controlled electronically within 0.1 percent. The load applied by the hydraulic piston was measured to ± 50 N, using a high precision force sensor. Vibration spectra and shaft orbits were measured with eddy current noncontacting transducers, connected to a dynamic data acquisition instrument.

The location of the thermocouples in the HSS bearings is shown in Figures 3 and 4. One hundred and seventeen thermocouples (1.0 mm diameter, chromel-alumel) were used. Eighty-four of them were located both circumferentially and axially at the internal pad surfaces, the active part of these thermocouples was flush to the pad surface and in contact with the fluid film. For each bearing, four thermocouples measured the temperature at

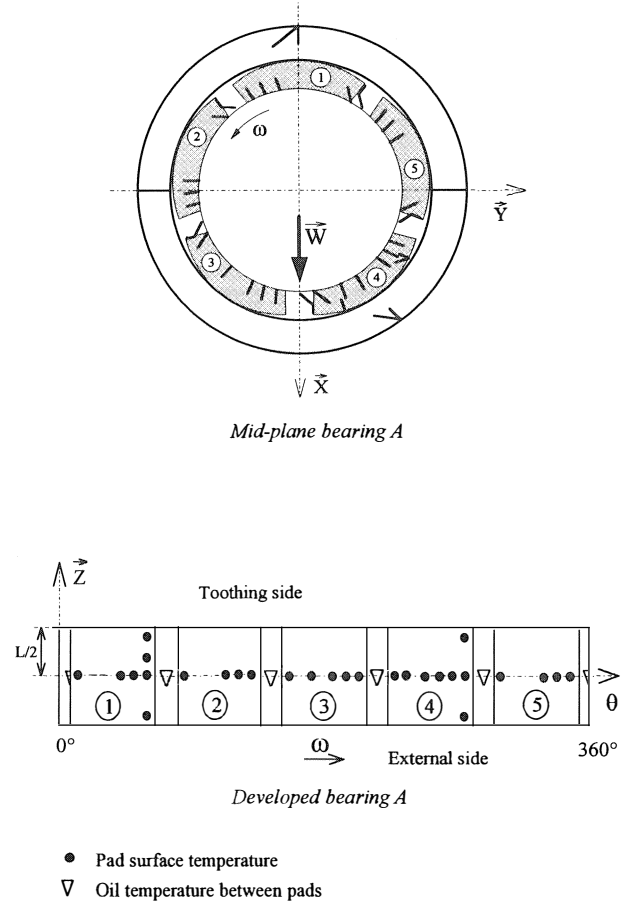


Figure 3. Location of Thermocouples in Bearing A.

Table 2. LSS Bearing Geometry and Operating Conditions.

		Bearing D (position 1)	Bearing E (position 2)
Number of pads		2	2
Journal diameter	(m)	0.23	0.23
	in	9.055	9.055
Bearing length	(m)	0.175	0.175
	in	6.889	6.889
Radial bearing clearance	(m)	$0.17 \cdot 10^{-3}$	$0.17 \cdot 10^{-3}$
	in	0.0669	0.0669
Lobe thickness	(m)	$41 \cdot 10^{-3}$	$41 \cdot 10^{-3}$
	in	1.614	1.614
Load direction		Middle of lobe 1	50° of trailing edge
Lobe arc angle	(°)	160	160
Applied load	(kN)	0 to 100	0 to 100
	lb	zero to 22,000	zero to 22,000
Range of speed	(rpm)	0 to 3366	0 to 3366
Oil inlet temperature	(°C)	50 and 72	50 and 72
	°F	122 and 161.6	122 and 161.6
Feeding pressure	(Mpa)	0.1	0.1
	psi	14.5	14.5

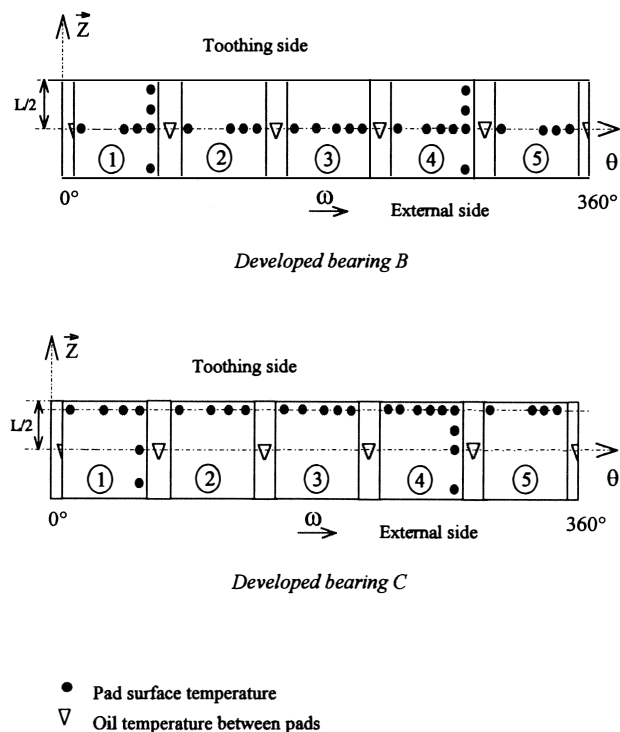


Figure 4. Location of Thermocouples in Tilting-pads Journal Bearings B and C.

half thickness and on the back of the pads. The other thermocouples were located in the housing and in the oil space between pads at 2.0 mm from the shaft surface. The design of bearing C (spherical pivot on the back of the pads), prevented placement of the thermocouples in the mid-plane. Only two thermocouples give circumferential temperature profiles in the mid-plane of pads number 1 and 4 at 90 percent of their circumferential amplitude. The remaining thermocouples are located on the external side of the bearing and between pads.

The location of the thermocouples in the LSS bearings is shown in Figure 5. Thirty-six were located circumferentially and axially at the internal pad surfaces, the active part of these thermocouples was also flush to the pad surface and is in contact with the fluid film. For one of the bearings, two thermocouples measured the temperature at half thickness of the bush.

The temperature accuracy is $\pm 0.5^\circ\text{C}$. The lubricant used was a standard ISO VG 32 mineral oil for which the temperature-viscosity variation was assumed to be exponential.

EXPERIMENTAL PROGRAM

The experimental apparatus was operated between 2700 rpm and 11,880 rpm for HSS bearings, i.e., the linear velocity varied from 22 m/s to 100 m/s. For LSS bearings, the rotational speed varies from 765 rpm (9 m/s) to 3366 rpm (40 m/s). The range of the test bearing specific load was up to 3.5 MPa for all the configurations studied. Specific loads are based on the total applied load and the projected area of the bearings (axial length times shaft diameter). The measurements were performed under steady-state conditions. After thermal equilibrium is reached, data were recorded, usually in about half an hour. For a given speed, a constant load is applied step by step from 0 to 88 kN for HSS bearings and from 0 to 100 kN for LSS bearings. The temperature of the feeding lubricant was kept constant and equal to 50°C .

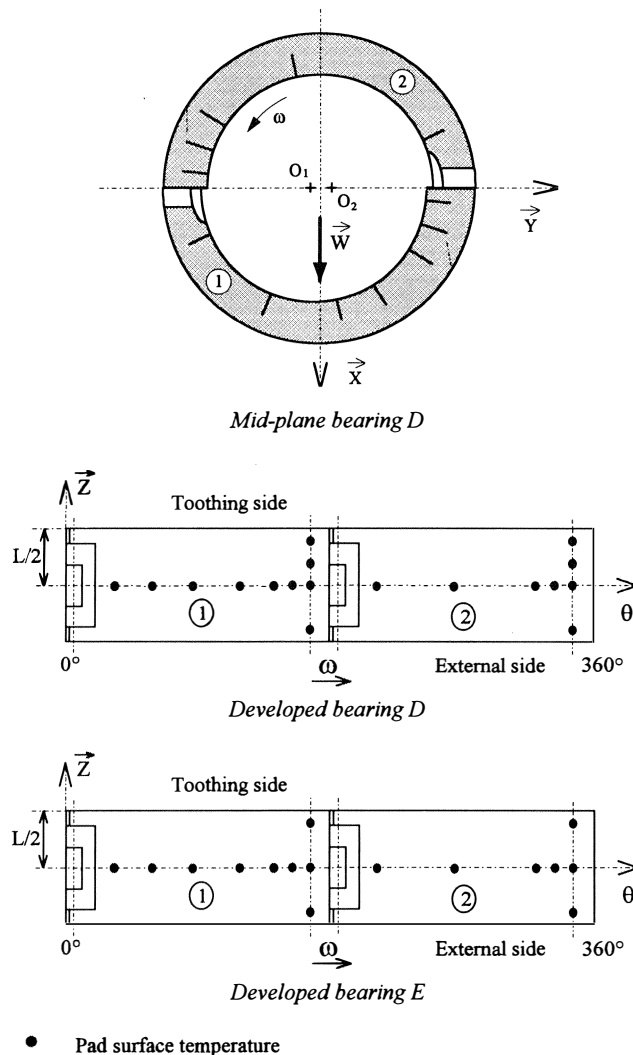


Figure 5. Location of Thermocouples in Offset-halves Journal Bearings D and E.

EXPERIMENTAL RESULTS

Discussion on Temperatures Measured in High Speed Shaft (HSS) Test Bearings

Circumferential temperature profiles of the internal pad surface for three bearings are presented in Figures 6, 7, 8, and 9. In these figures, the bearings are developed and the load direction is vertical between pads number 3 and 4. For bearing C (Figure 9), the thermocouples are not located in mid-plane for obvious reasons of conception (spherical pivot on the back of the pads).

For all operating conditions, the maximum temperatures are set in a zone between 70 and 90 percent of pad length and the lowest temperatures are set at the pad leading edge. For the unloaded case (Figure 6), the difference between maximum temperatures of each pad for a given speed, is less than or equal to 3.0°C . For the loaded cases (Figures 7 to 9), temperatures are not symmetrical. Temperatures of high loaded pads (number 3 and 4) are greater than the low loaded pads (number 1, 2 and 5). Because the shaft eccentricity is large, it induces a decrease in loaded-pad film thickness and an increase in the film thickness of the unloaded pad. Thus, the heat flux recirculations carried from one pad to another are not the same for all the pads. Moreover, the fall of temperatures in pad trailing edge is more

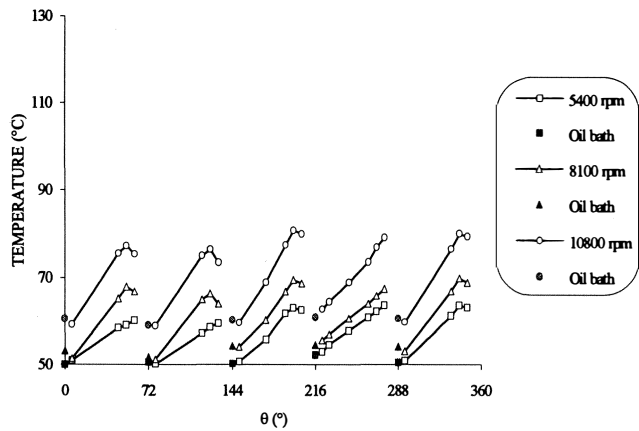


Figure 6. Internal Pad Surface Temperatures of Bearing A Vs Angular Coordinate, for Different Speeds ($W = 0$ kN).

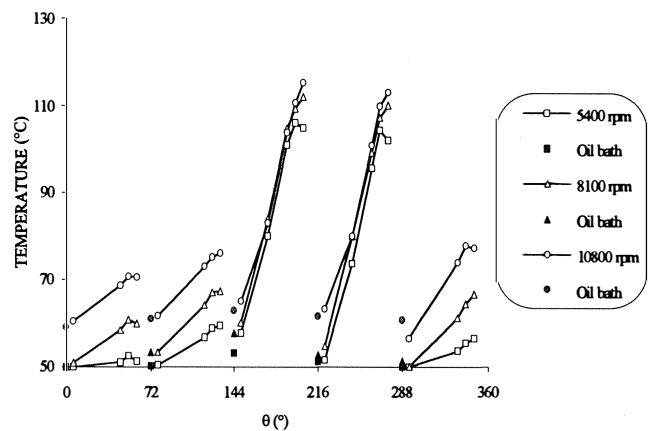


Figure 8. Internal Pad Surface Temperatures of Bearing B Vs Angular Coordinate, for Different Speeds ($W = 88$ kN).

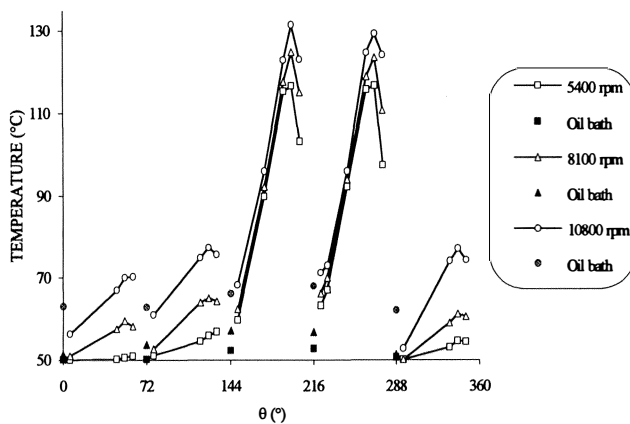


Figure 7. Internal Pad Surface Temperatures of Bearing A Vs Angular Coordinate, for Different Speeds ($W = 88$ kN).

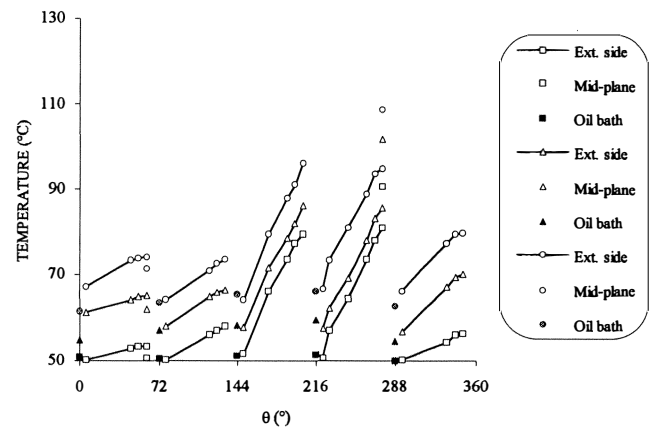


Figure 9. Internal Pad Surface Temperatures in Mid-plane and on External Side of Bearing C Vs Angular Coordinate, for Different Speeds ($W = 88$ kN).

marked on bearing A, for which the pivots are centered. This is due to the pivot angular positions : when the α/β ratio is higher than 0.5, the minimum film thickness is reduced. For the offset pad pivot bearings B and C, film thickness and therefore circumferential flowrate at the trailing edge of pad number 3 become low; consequently, the requirement of fresh fluid is more important than for the bearing A case.

The fluid temperature in the space between pads near the shaft is also noted in Figures 6, 7, 8, and 9. For the case presented in Figure 9, all these temperatures are approximately identical at 2.0°C ; for a given applied load, they increase with the rotational speed. When the bearing is loaded, the oil temperatures between pads vary as the maximum babbitt temperatures vary. The maximum oil temperature between pads is always situated above pad number 3 and the minimum one above pad number 5. This is due to the quantity of heat flux carried over from one pad to the next.

In order to compare the types of bearings, the maximum babbitt temperatures vs rotational speed, at nominal load (88 kN) are presented in Figure 10. Whatever the rotational speed, the "coolest" bearing is bearing C, for which the pads are made in copper-bronze alloy with spherical offset pivots ($\alpha/\beta = 0.6$). At nominal operating conditions ($N = 10800$ rpm $W = 88$ kN), maximum temperature is about 110°C . The greatest temperatures are obtained for the bearing A, for which the pad pivots are centered ($\alpha/\beta = 0.5$); for this configuration, the maximum temperature is 131°C . For nominal conditions, shifting the pivot

from the central position to at the least 55 percent position, leads to a decrease of the maximum temperature of about 15°C . For the centered pad pivots (bearing A), temperature varies more with the rotational speed (65 percent) than with the applied load (35 percent). For offset pad pivots (bearings B and C), temperatures are identically influenced by both load and rotational speed.

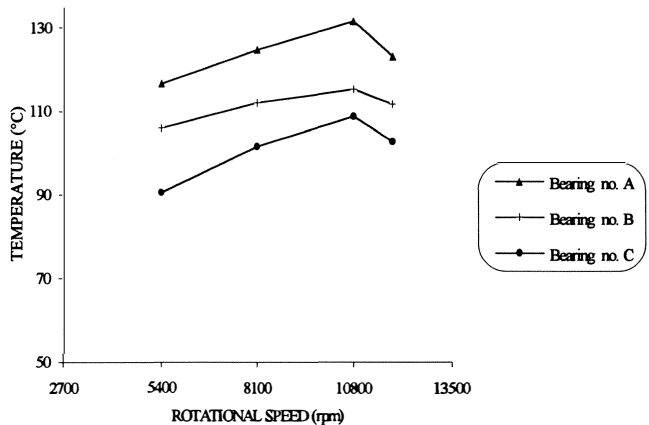


Figure 10. Maximum Babbitt Temperature Vs Rotational Speed ($W = 88$ kN).

As some authors have already emphasized [3, 6, 10], for high peripheral speeds ($\geq 90\text{m/s}$), a reduction of the maximum temperature, due to the change in flow regime from laminar to turbulent is also noted. Indeed, theoretical calculations have shown that the local Reynolds number is about 1800 and the Taylor number is about 100. This phenomenon has been explained by the velocity profile [12, 13, 14]: under turbulent flow regime, the shear stresses are low in the central zone of the film and are very high near the walls. The turbulent effects tend to homogenize the temperature into the film. At the film/shaft and film/pad interfaces, the temperature gradients across the film thickness are very large and induce a very low temperature of the babbitt.

The temperature variation across the thickness of the pad with the highest loaded pad thickness is measured for each bearing. The temperatures of bearing A on the internal pad surface, at half-thickness and on the back of pad number 4 are given vs rotational speed in Figure 11. The temperatures are measured both on the leading and trailing edge at nominal load (88 kN). The thermocouples are located in the mid-plane at 10 and 85 percent of circumferential pad length. Generally, the temperature variations at half-thickness are similar to the ones on the internal pad surface. The temperature gradient in the pad at the leading edge is lower than the one observed in the pad at the trailing edge. At the inlet region, the temperature in the pad is only slightly influenced by the rotational speed because in this zone, the pad temperature is strongly dependent on the supply temperature. On the other hand, in the pad exit region, the temperature increases with the rotational speed, then drops when the flow regime becomes nonlaminar.

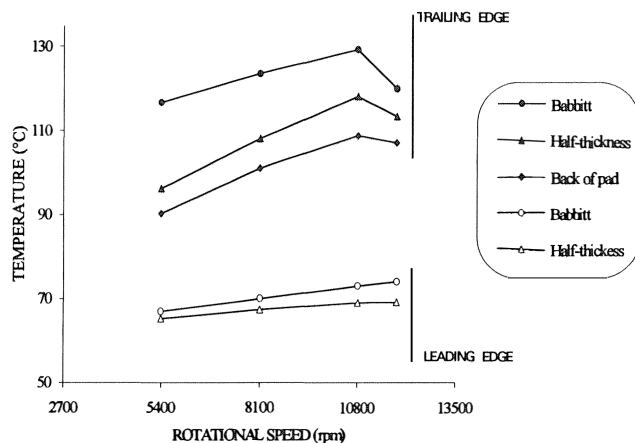


Figure 11. Temperatures of the Internal Pad Surface, Half-thickness and Back of Pad Number 4 (Bearing A), for Different Speeds ($W = 88\text{ kN}$).

The axial variation of the surface temperature of the high loaded pad of bearing B is given in Figure 12 for a rotational speed of 10,800 rpm. In this figure, the abscissa 80 millimeters is located in the mid-plane bearing. This temperature remains almost constant when the load is nil [15]. For large loads, the results agree with the prediction; the maximum temperature is situated in the mid-plane of the bearing. The difference in measured temperature between the extremities and the mid-plane of the pad can reach 20°C . The babbitt temperature on the tooth side is always higher than that measured on the external side; this discrepancy of temperature is probably due to the heating in the gearing. The same tendencies are noted for both bearings B and C.

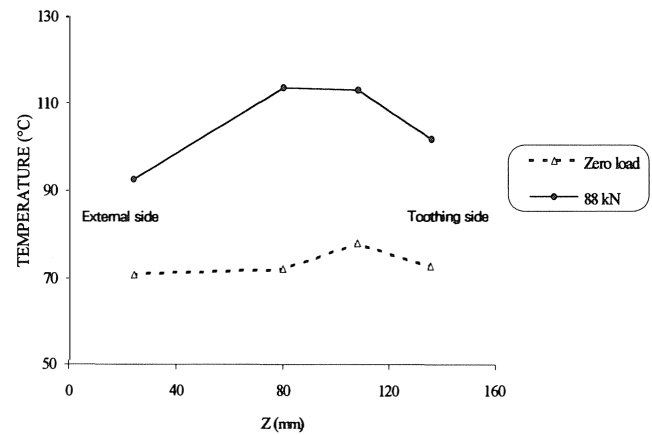


Figure 12. Axial Variation of Internal Pad Surface Temperatures (Pad Number 4, Bearing B) at 90 Percent of Circumferential Pad Length, for Different Load ($N = 10,800\text{ rpm}$).

In Figure 13, circumferential temperature profiles of the internal pad surface for both 50°C and 72°C inlet lubricant temperature are presented for nominal operating conditions. Whatever the operating conditions, babbitt temperatures follow a similar evolution along the circumferential direction. However, the difference of the maximum temperatures (16°C) is lower than that at the leading edge (21°C).

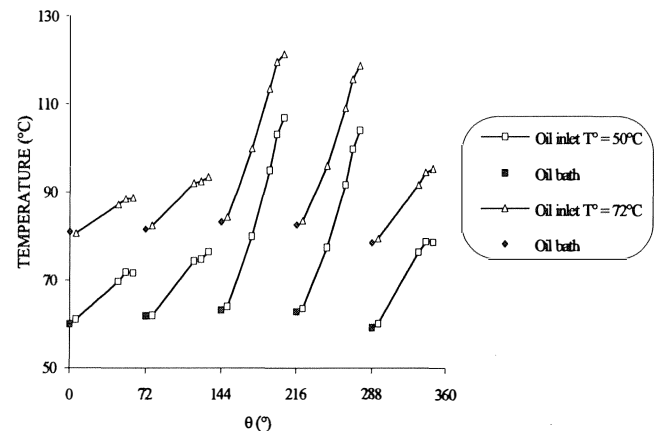


Figure 13. Internal Pad Surface Temperatures of Bearing B Vs Angular Coordinate, at Nominal Operating Conditions ($N = 10,800\text{ rpm}$; $W = 88\text{ kN}$).

Discussion on Power Loss Measured in HSS Test Bearings

The power loss variation vs rotational speed is presented in Figure 14. The power loss evolution is a quadratic form vs rotational speed and linear vs applied load for a given rotational speed. Generally, the applied load has a smaller influence on bearing power loss than the rotational speed, which accounts for 80 percent of total power loss, within the limits of the experimental work. For power loss evaluation, the average temperatures of the supplied oil and the drain are used. It is assumed that 85 percent of heat generated by shearing in the fluid is evacuated by the fluid. For these tests, oil required for each bearing is adjusted with the help of caliber nozzles. At 75 percent of rotational speed and beyond, the oil flowrates for bearings A, B and C are, respectively, 155, 165, and 130 l/min. Under these conditions, the lowest power loss is obtained with bearing C

(spherical pivots), followed by center and offset pivot bearings. However, power loss obtained for copper-bronze bearing C must be read with caution. As for the other bearings, it is supposed that 85 percent of heat was dissipated by lubricant; but, copper-bronze alloy has a thermal conductivity nine times greater than steel and enables heat to be dissipated more readily from the bearing surface.

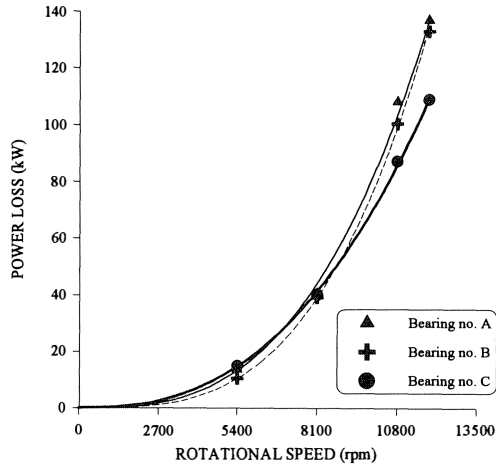


Figure 14. Power Loss Vs Rotational Speed for Bearings A, B, and C ($W = 88$ kN).

Discussion on Temperatures Measured in Low Speed Shaft (LSS) Test Bearings

Initially, offset-halves bearings are loaded in the middle of a lobe. In order to minimize the temperature and power loss, other loading configurations have been studied, notably in applying the load toward the trailing edge of the lobe. Circumferential temperature profiles of the internal lobe surface of the bearing D are presented in Figures 15 and 16. The bearing is developed and the load direction is vertical in the middle of the lobe 1. For all operating conditions, the maximum temperatures are set in a zone between 80 and 90 percent of the lobe length. With regard to low loaded lobe, the maximum temperature is situated at the extremity of lobe. Babbitt temperatures at the leading edge of the lobes are always inferior or equal to 60°C . For a zero external load (Figure 15), the values of the maximum temperature on the two lobes are different because of the weight of the rotor (1,9

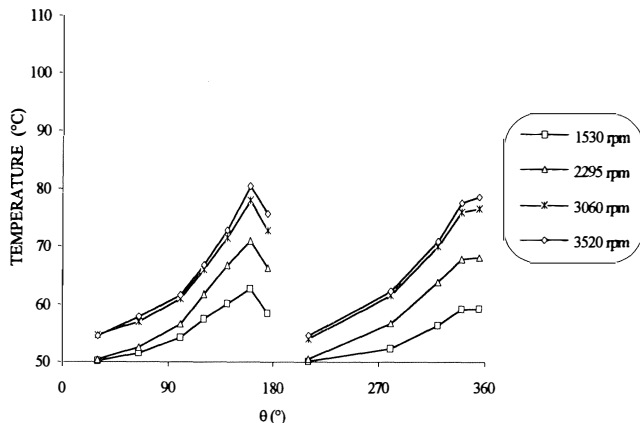


Figure 15. Internal Lobe Surface Temperatures of Bearing D Vs Angular Coordinate, for Different Speeds ($W = 0$ kN).

kN). This difference of temperature decreases when the rotational speed increases because the shaft tends to center in the bearing due to the hydrodynamic effect. For the loaded cases (figure 16), the maximum temperature is situated in the same zone as that observed for the unloaded case under all operating conditions. The difference in maximum babbitt temperatures between loaded and unloaded lobe can reach 25 to 30°C . The same tendencies for bearing E are also noted.

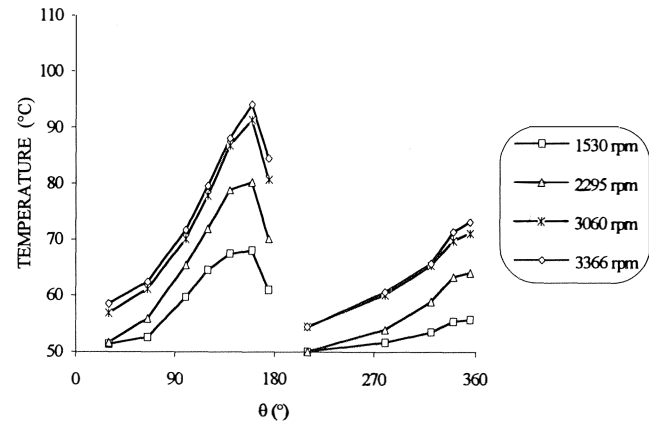


Figure 16. Internal Lobe Surface Temperatures of Bearing D Vs Angular Coordinate, for Different Speeds ($W = 100$ kN).

The maximum babbitt temperature vs rotational speed for a load up to 10 kN is presented in Figure 17. In this bearing, evolution of maximum babbitt temperature vs rotational speed and load is almost linear, with a slight falling in overspeed. Generally, the rotational speed has a greater influence on bearing temperature than the applied load, which accounts for 30 percent for the bearings tested and with the limits of the experimental work.

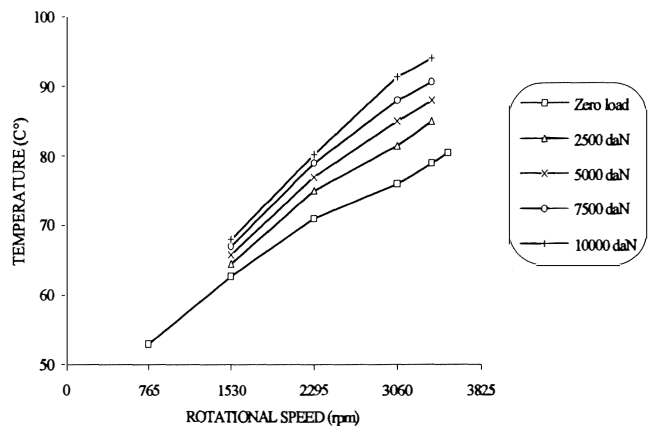


Figure 17. Maximum Babbitt Temperature of Bearing D Vs Rotational Speed and Load.

In order to study the influence of load direction, babbitt temperature vs angular coordinate at nominal operating conditions is presented in Figure 18. If the bearing split joint is inclined so that the load is applied 50 degrees before the trailing edge of lobe 1 (position 2), the maximum babbitt temperature decreases 5°C compared to the uninclined position, in which the load is applied in the middle of lobe 1 (position 1). This

temperature decrease is probably due to the increase film thickness, which is more important when the load is applied at 50 degrees from the trailing edge of lobe 1. Because the average Reynolds number is about 900, it is possible that the bearing may be in transition between the laminar and turbulent flow regimes. This phenomenon facilitates mixing of the lubricant in the leading edge zone and contributes in this way to a decrease in babbit temperature.

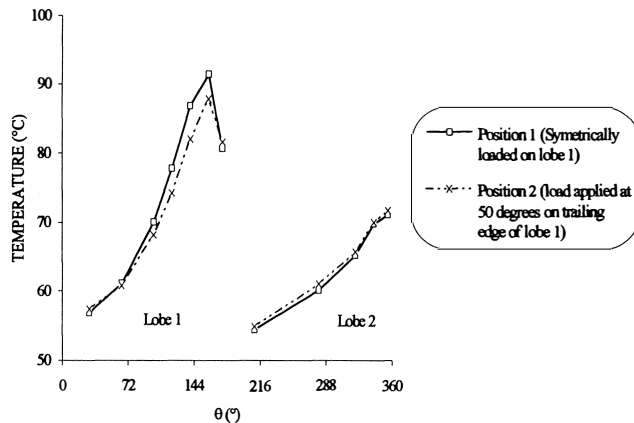


Figure 18. Influence of Load Direction on Bearing D Vs Angular Coordinate, at Nominal Operating Conditions ($N = 3060$ rpm; $W = 100$ kN).

In Figure 19, circumferential temperature profiles of the internal lobe surface for both 50°C and 72°C inlet lubricant temperature are presented for nominal operating conditions. Whatever the operating conditions, babbit temperatures follow a similar evolution along the circumferential coordinate. However, as in tilting-pad journal bearings, the difference of the maximum temperatures (11°C) is lower than that at the leading edge (21°C). Thus, the decrease in feeding temperature (22°C) permits a maximum temperature reduction of only 10°C.

Discussion on Power Loss Measured in LSS Test Bearings

It has just to be shown that if the bearing split joint is inclined so that the load is applied 50 degrees before the trailing edge of lobe 1, the maximum babbit temperature decreases 5°C com-

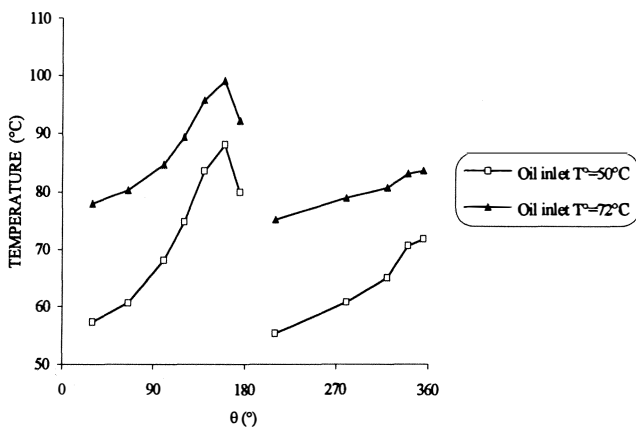


Figure 19. Internal Lobe Surface Temperatures of Bearing D Vs Angular Coordinate, at Nominal Speed ($N = 3060$ rpm) and a Load of 75 kN.

pared to the position 1. This arrangement reduces the power loss by 7.0 percent (Figure 20) for nominal operating conditions ($N = 3060$ rpm; $W = 100$ kN) and slightly decreases, for these same conditions, the oil flowrate (4.0 percent), because of a lower eccentricity and a greater attitude angle.

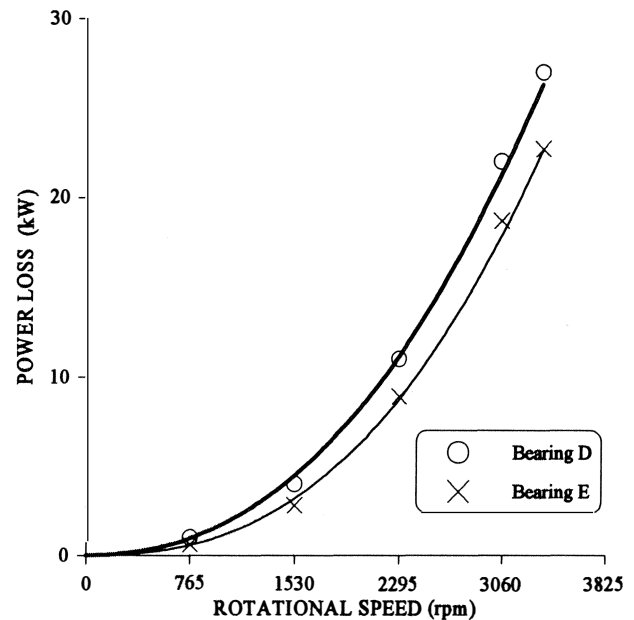


Figure 20. Power Loss Vs Rotational Speed for Bearings D and E ($W = 100$ kN).

COMPARISON BETWEEN THEORETICAL RESULTS AND EXPERIMENTAL DATA

High Speed Rotor Bearings.

The theory for the tilting-pad journal bearing has been presented by Fillon and Frêne[16]. The thermal and elastic problems are solved in the mid-plane bearing assuming that the axial variation of both temperatures and solid displacements is very small and can be neglected. In a first part, Figure 21 presents both theoretical and experimental temperatures of the internal pad surface for bearing A. The nominal operating conditions ($N = 10,800$ rpm $W = 88$ kN) are applied. Generally, experimentally measured temperatures on the internal pad surface are always higher than those predicted by the theoretical model. However, the general form of curves are rather similar. On the other hand, the drop of experimental temperatures on pad trailing edge is not shown. Large differences are noted between thermohydrodynamic results (THD) obtained without deformations and experimental data, in particular on unloaded pads for which the discrepancy reaches 10°C. The theoretical results including thermoelastic displacements (TEHD) of bearing elements provide reasonable temperature predictions for the unloaded pads, but for the highly loaded pads the maximum temperature decreases about 6°C. Indeed, the thermoelastic displacements induce a decrease of the bearing clearance, and, consequently, a decrease of the eccentricity; this also leads to a very small film thickness on the low loaded pads. When thermoelastic displacements are taken into account, the pad distortion modifies the film geometry and increases the internal pad radius. In addition, the thermal expansion of shaft, pads and housing reduces the operating bearing clearance [17]. Finally, the expansion of the inferior gear-unit casing and of the bearing-cap, along with the ambient temperature around the formal bearings, have certainly

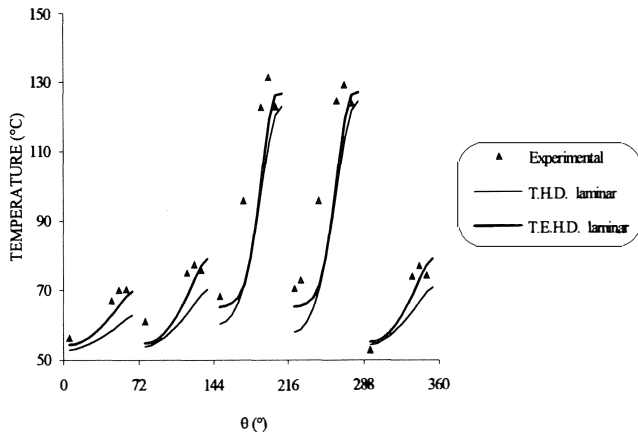


Figure 21. Experimental and Theoretical Temperatures of the Internal Pad Surface of Bearing a ($N = 10,800$ rpm; $W = 88$ kN).

a marked effect. These specific parameters are not taken into account in the theoretical model.

The maximum temperature measured on the internal pad surface of bearings A and B are greater than predicted with the TEHD model (Figure 22), except at the highest rotational speeds. For very high speeds (>90 m/s), the theoretical model predicts greatest temperature due to the assumption of a laminar flow regime. The drop of maximum temperature resulting from the change in flow regime which is shown experimentally cannot be obtained using this assumption. For a laminar flow regime (<90 m/s), the temperature discrepancy between theoretical results and experimental data is all the smaller as the rotational speed is high. Concerning bearing C, the maximum temperature predicted by the theoretical model is always over-estimated whatever the rotational speed. This temperature discrepancy can be explained by the effect of the spherical pivots, which permit a better flow of fresh fluid on the back of the pads. This phenomenon tends to cool the pads. In addition, the "pumping" of this heat by the lubricant is facilitated by the copper-bronze alloy,

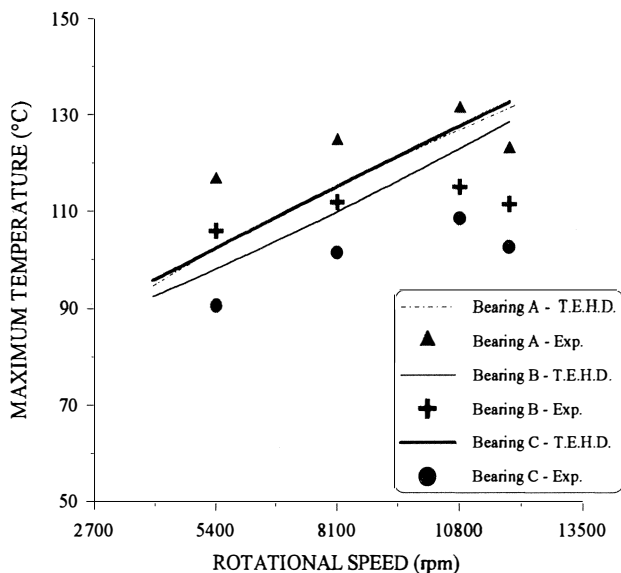


Figure 22. Experimental and Theoretical Maximum Babbitt Temperatures Vs Rotational Speed, for Bearings A, B and C ($W = 88$ kN).

which has a greater thermal conductivity than steel. This cooling effect is not taken into account in the numerical model.

The power loss variation is given in Figure 23 vs the rotational speed for the three journal bearings. The good agreement between theoretical and experimental results is obtained as long as the rotational speed is not too high. As expected, the power losses become very large for the highest rotational speeds due to the flow nonlaminar regime. For high operating speeds, the discrepancy can result from two effects which are not taken into account in the numerical program:

- existence of a laminar to turbulent transition flow regime in the film,
- the power loss due to the churning oil in the space between pads, which can be very large.

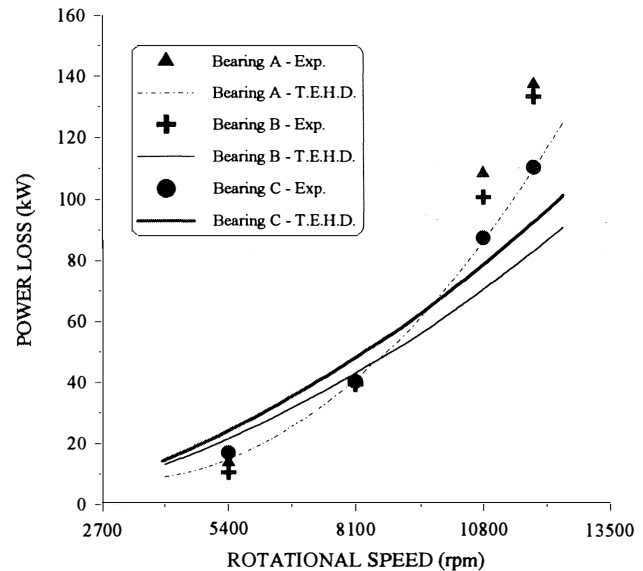


Figure 23. Experimental and Theoretical Power Losses Vs Rotational Speed, ($W = 88$ kN).

Low Speed Rotor Bearings

The theoretical study of these bearings is performed using both the CEMTH7 [16] and ALP3T [18] programs, in the thermohydrodynamic regime (THD). In the first part, both theoretical and experimental temperatures of the internal lobe surface of bearing E is presented in Figure 24. The nominal operating conditions are applied ($N = 3060$ rpm; $W = 100$ kN). Maximum temperatures obtained with the help of two programs are very near the experimental results. For this type of loading, maximum babbitt temperature is situated in a zone between 80 and 90 percent of circumferential amplitude of the lobe. The temperatures obtained by the CEMTH7 and ALP3T programs are very close to the experimental measurement along lobe 1. However, a temperature discrepancy on unloaded lobe 2 of about 15 degrees below the experimental values is noted. Two reasons can explain this difference of temperature. First thermoelastic deformations are not taken into account in theoretical models. Second, the theory predicts cavitation in the divergent portion of the lobe 2, which induces an axial "pumping" effect. Because in a real bearing, this cavitation causes hot oil adhering to the shaft to enter the lobe clearance, increasing the babbitt temperature.

For this type of bearing, oil flowrate is influenced very little by load direction. In this way, evolution of oil flowrate vs

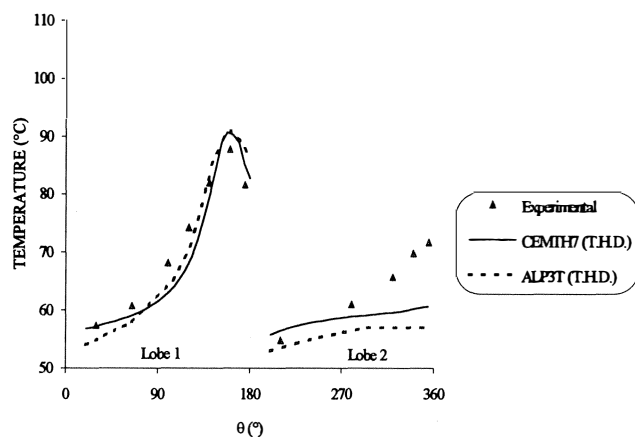


Figure 24. Experimental and Theoretical Temperatures of the Internal Lobe Surface of Bearing E ($N = 3060$ Rpm; $W = 100$ kN).

rotational speed (bearing E), for a nominal load of 100 kN is shown in Figure 25. For a range of speeds between 765 and 2295 rpm, oil flow calculated with CEMTH7 and ALP3T programs are in good agreement with measured oil flow. It should be observed that in CEMTH7 program, only axial oil flow on a level of active surfaces is taken into account. It would have in fact added more flowrate coming out axially of supply grooves, because for low speed this flowrate is predominant. Finally, evolution of the calculated oil flowrate is linear vs rotational speed, while experimentally, a falling of the curve is recorded after 2295 rpm. This phenomenon can result in a reduction of operating bearing clearance for high rotational speed, due to differential expansion of bearing elements.

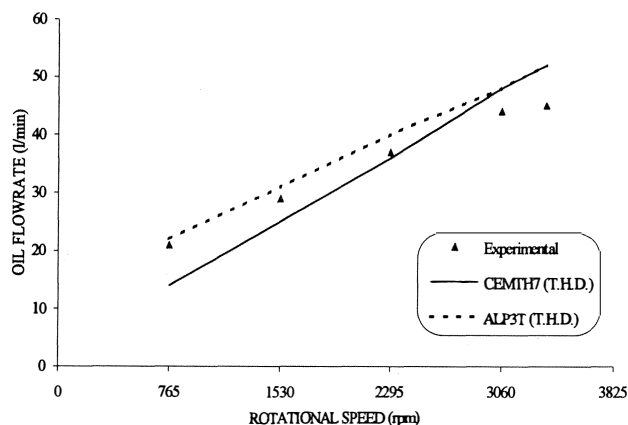


Figure 25. Experimental and Theoretical Oil Flowrate Vs Rotational Speed, for Bearing E ($W = 100$ kN).

For power loss evaluation, the average temperatures of the supplied oil and the drain are computed as for tilting-pads journal bearings. The power loss variation vs rotational speed for a constant load, applied at 50 degrees on trailing edge (bearing E), is presented in Figure 26. The power loss evolution is a quadratic form vs rotational speed, with a good agreement of results until 75 percent of rotational speed. Beyond this speed, predicted power loss by the theoretical models is under-estimated by about 45 for the bearings tested. These important gaps are partly due to the fact that thermoelastic displacements are not taken into account in theoretical models. Moreover, theoretical

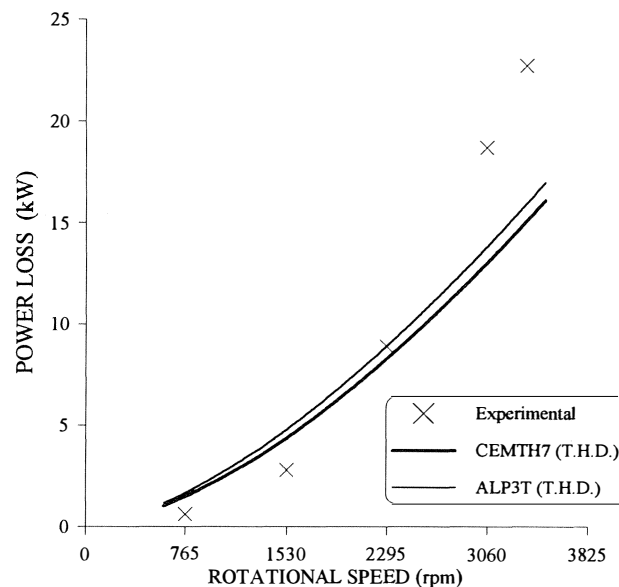


Figure 26. Experimental and Theoretical Power Losses Vs Rotational Speed, for Bearing E ($W = 100$ kN).

calculations have shown that the average Reynolds number is about 900, this would let to suppose that the bearing is situated in a transition flow regime from laminar to turbulent. So these two phenomena would contribute in an increase of power loss. In addition, frictional losses in the supply groove, which can be important, are not taken into account in the theoretical models.

CONCLUSION

The experimental test device recreating speed and load conditions usually applied onsite has been used to investigate the conditions permitting the reduction of the babbitt temperatures of tilting-pad journal bearings. From these experimental results, the following concluding remarks can be drawn:

- Shifting the pivot from the central position to at least the 55 percent position leads to a decrease of the maximum temperature of about 15°C and to a decrease in the power loss (-10kW), for nominal operating conditions.
- Decreasing the oil inlet temperature from 72 to 50°C does not significantly reduce the maximum babbitt temperature; for nominal operating conditions, the drop of the maximum temperature is only 10°C.
- The bearing design and materials, such as bearing C, for which the pads are made in copper-bronze alloy, with spherical offset pivots, contribute to improve its performance, notably temperature (21°C at nominal conditions) and power loss.
- Under high linear speeds (≥ 90 m/s), a reduction of the maximum temperature is noted due to the change in flow regime from laminar to turbulent. This also tends to increase the power loss.
- The comparison between theoretical results and experimental data show that the T.H.D. analysis alone is not sufficient to predict bearing performance. The displacements of all the bearing elements (TEHD) have to be taken into account in order to define the operating bearing clearance and internal pad surface distortion. For very high speed, it is necessary to take into account the change in flow regime to predict accurately the bearing performance.
- For offset-halves bearings, applying load at 50 degrees from the trailing edge of a lobe permits reduction from of both

the maximum babbitt temperature and the power loss of the bearing compared to the case in which the load is applied in the middle of a lobe.

REFERENCES

1. Dmochowski, W. and Brockwell, K., "Calculation and Measurement of Steady State Operating Characteristics of the Five Shoe, Tilting-Pad Journal Bearing," Proc. Of the 5th Int. Cong. On Tribology, Eurotrib, 3, pp.168-173 (1989).
2. Fillon, M., Souchet, D., and Frene, J., "Influence of Bearing Element Displacements on Thermohydrodynamic Characteristics of Tilting-Pad Journal Bearings," Int. Tribology Conf., ITC Nagoya, pp. 635-639 (1990).
3. De Choudhury, P. and Masters, D. A., "Performance Tests of Five-Shoe Tilting-Pad Journal Bearing," ASLE Transactions, 27, pp. 61-661 (1984).
4. Brockwell, K. and Kleinbub, D., "Measurement of Steady State Operating Characteristics of the Five-Shoe, Tilting-Pad Journal Bearing," Tribology Transaction, 32, pp. 267-275 (1989).
5. Hopf, G. and Schüller, D., "Investigations on Large Turbine Bearings Working Under Transitional Conditions Between Laminar and Turbulent Flow," ASME Journal of Tribology, 111, pp. 628-634 (1989).
6. Taniguchi, S., Makino, T., Takeshita, K., and Ichimura, T., "A Thermohydrodynamic Analysis of Large Tilting-Pad Journal Bearing in Laminar and Turbulent Flow Regimes with Mixing," ASME Journal of Tribology, 112, pp.542-548 (1990).
7. Harangozo, A. V., Stolarski, T. A., and Gozdawa R. J., "The Effect of Different Lubrication Methods on the Performance of a Tilting-Pad Journal Bearing," STLE Tribology Transactions, 34, pp. 529-536 (1991).
8. Tanaka, M., "Thermohydrodynamic Performance of a Tilting Pad Journal Bearing with Spot Lubrication," ASME Journal of Tribology, 113, pp. 615-619 (1991).
9. Fillon, M., Bliglout, J. C., and Frene, J., "Experimental Study of Tilting-Pad Journal Bearings—Comparison with Theoretical Thermoelastohydrodynamic Results," ASME, Journal of Tribology, 114, pp. 579-588 (1992).
10. Simmons J. E. L. and Dixon S. J., "Effect of Load Direction, Preload, Clearance Ratio and Oil Flow on the Performance of a 200 mm Journal pad Bearing," Tribology Transactions, 37, pp. 227-236 (1994).
11. Gardner, W. W. and Ulschmid, J. G., "Turbulence Effects in Two Journal Bearing Applications," ASME Journal of Lubrication Technology, 96, pp. 15-21 (1974).
12. Bouard, L., Fillon, M., and Frene, J., "Comparison Between Three Turbulent Models—Application to Thermohydrodynamic Performance of Tilting-Pad Journal Bearings," Proc. of the 4th Int. Trib. Conf. Austrib, 1, pp. 119-125 (1994).
13. Constantinescu, V. N., "Basic Relationships in Turbulent Lubrication and Their Extension to Include Thermal Effects," ASME Journal of Lubrication Technology, 95, pp. 147-154 (1973).
14. Ha, H. C., Kim, H. J., and Kim, K. W., "Inlet Pressure Effects on the Thermohydrodynamic Performance of Large Tilting Pad Journal Bearing," preprint 94-Trib-26, ASME/STLE Tribology Conference, Maui, Hawaii, pp. 1-6 (1994).
15. MAAG Gear Company Ltd., "High speed Gears—New Development," 3ème Congrès Mondial Sur les Engrenages et Transmissions (CMET), Paris (1992).
16. Fillon, M. and Frene, J., "Numerical Simulation and Experimental Results on Thermoelasto-Hydrodynamic Tilting-Pad Journal Bearings," IUTAM Symposium on Numerical Simulation of Nonisothermal Flow of Viscoelastic Liquids, Kerckrade, Neederlan, November 1993, Kluwer Academic Publishers, Dordrecht, pp. 85-89 (1994).
17. Fillon, M., Frene, J., and Boncompain, R., "Etude Expérimentale de L'effet Thermique Dans les Paliers à Patins Oscillants," Proc. Eurotrib, 1, p. 4.1.6 (1985).
18. Mittwollen, N. and Glienicke, J., "Operating Conditions of Multi-lobe Journal Bearings under High Thermal Loads," Transaction of the ASME, 112, pp. 330-340 (1990).

